Journal of Process Control 24 (2014) 1023–1037

Contents lists available at ScienceDirect

Journal of Process Control

journal homepage: www.elsevier.com/locate/jprocont

Feedback PID-like fuzzy controller for pH regulatory control near the equivalence point

M.C. Heredia-Molinero [a], J. Sánchez-Prieto [c], J.V. Briongos [c,*], M.C. Palancar [b]

[a] Universidad Politécnica de Madrid, Escuela Universitaria de Ingeniería Técnica de Obras Públicas, C/ Alfonso XII, 3 y 5, Madrid, Spain
[b] University Complutense of Madrid, Facultad de Ciencias Químicas, Departamento de Ingeniería Química, Avda. Complutense S/N, 28040 Madrid, Spain
[c] Universidad Carlos III de Madrid, Escuela Politécnica Superior, Departamento de Ingeniería Térmica y de Fluidos, Avenida de la Universidad 30, 28911 Leganés, Madrid, Spain

ARTICLE INFO

Article history:
Received 27 June 2013
Received in revised form 7 May 2014
Accepted 7 May 2014

Keywords:
pH control
Fuzzy logic
Process control
Wastewater treatment

ABSTRACT

In this research the use of a feedback PID-like fuzzy controller scheme for pH control is presented to deal with instability problems near the equivalence point in neutralization processes. State space analysis of the titration curves and a fuzzy clustering algorithm based on calculating a measure of potential derived from the square distance of the pH data are complementary applied to define the membership structure and the fuzzy sets of the controller. To test the performance of the controller, both simulated and experimental runs were used. The fuzzy controller was tested for compensating step-change perturbations of propionic acidic flow rates, propionic acid concentration, and buffering conditions. Stationary cycling behavior has been observed for large loads of acidic flow rates. It was found that though the rejection time was strongly dependent on the mean residence time of the liquid solutions, the proposed controller keep the neutralization process operating close to the specified set point of pH = 7.

1. Introduction

Due to the significant effect of the pH value on life ($pH = -\log[H^+]$), environment, matter and kinetics, its control is a necessary common practice in both chemical and biochemical industrial processes. However, the inherent nonlinear nature of the titration curves associated to the different acid–base reaction systems makes pH control near to the points of inflection of the corresponding titration curves an intricate problem. Moreover, the challenge of controlling the pH value grows in industrial applications due to the unavoidable fluctuations suffered by the process operational conditions, and the issues regarding the pH measurement process such as: time lag and dead zones, accuracy, noise, residence time for the liquid flows. As a result, it can be found in literature a large research effort addressed to pH control where the number and type of control techniques applied is diverse. Accordingly, there are many examples of linear [1–7] as well as nonlinear approaches [8–11].

The main drawbacks exhibited by either linear and nonlinear methods lies on the consistency of the model as well as on the tuning parameters, and the subsequent sustenance of the proper control action to fulfill the process needs during common operation with variations in the operational conditions. Among the nonlinear approaches, the promising result obtained through the use of Artificial Neural Networks (ANNs) [11,12] give rise to the development of research lines that explore the use of 'artificial intelligence' (AI) methods, that put together different techniques such as ANN's and Fuzzy logic to deal with the sensitivity problem near the inflection points [13–16]. Among the different nonlinear methods used in pH-control applications, the fuzzy logic techniques are aimed to mimic the performance of a skillful plant operator, and to that end the approach mix membership functions with logic rules. As a result the controller response is expected to be optimized for the operational conditions considered during the model development [17–19].

Although the first results reported in literature on fuzzy controllers applied to neutralization process were strongly based on simulated data, they give a preliminary impression of the expected performance of the fuzzy approach [20–22]. Later, some examples existing in literature used both simulated and experimental data for fuzzy controller design and optimization. Such approximation to the problem leads toward two different approaches: empirical based and fuzzy controller structures. Empirically based fuzzy

Abbreviations: AI, Artificial intelligence; ANN, Artificial neural network; CSTR, Continuous stirred tank reactor; fcm, fuzzy clustering method; LA, Lower action limit; LWL, Lower warning level; UA, Upper action limit; UWL, Upper warning level.

* Corresponding author. Tel.: +34 916248392; fax: +34 916248810.
E-mail address: jvilla@ing.uc3m.es (J.V. Briongos).

http://dx.doi.org/10.1016/j.jprocont.2014.05.006
0959-1524/

Nomenclature

e	pH error
E	normalized pH error
N_{fr}	number of fuzzy rules
OV	valve opening, %
P_i	potential value of cluster i
r_a	radius defining a neighborhood around the cluster center
$r_{(H)}$	reaction rate, s
t	time, s
u_i	numerical value for the scaled membership function i
V	titrant flow rate, mL/s

Greek letters

μ	degree of membership
σ_{abs}	mean absolute deviation
τ	characteristic time, s
τ_r	rejection time, s

Subscripts

sp	set point
t	current time step

controllers are subjugated to some kind of empirical constant and, therefore, it is difficult to assess whether the structure of the fuzzy controller and the controller performance can be scaled to other neutralization problems [5,13]. In contrast, the fuzzy controllers allow both to verify the fuzzy rule formulation as well as to test the membership structures used to implement the controller [23,24].

In a previous work [25] it was reported that when a PD-like fuzzy controller is used regulatory control of a similar buffering systems, the pH response to perturbations lead to overshoots greater than 3 pH units. However, an analogous PID-like structure succeeds in eliminating the offset the overshoots found in the response were below than 1 pH-unit for step perturbations lower than 50%. According to that, in this work it is tested the use of a feedback PID-like fuzzy controller near the equivalence point under buffering conditions to explore the feasibility of the fuzzy controller to be applied in neutralization process. Such scheme is able to deal with the instability problems exhibited by the corresponding titration curves to small perturbations on the hydrogen ion [H^+] near the inflection point. The state space analysis of the titration curves of the different buffering acidic liquid streams was used to test the reliability of the fuzzy controller, and fuzzy clustering algorithms are complementary used to design the structure of the fuzzy controller. The proposed fuzzy controller was tested against large perturbations with several solutions of acidic liquid streams (Table 1) and a tight control condition over the neutralization process was achieved for the neutralization settings explored.

2. Structure of the feedback PID-like fuzzy controller

As it is well known, fuzzy controllers are built by means of optimization algorithms based on the control operator experience and use fuzzy rules as the mechanism to compute the response of the control system to a given input, as well as to describe qualitatively the existing relationship between several variables. The operation of the fuzzy controller is currently described in terms of fuzzification, fuzzy processing and defuzzification. Consequently, the current input is expressed as linguistic term to be processed as a fuzzy input according to the set of rules and the membership functions defined in the controller, and to provide the fuzzy output that is subsequently defuzzified producing a real value that can be used as the controller output. Moreover, the fact that the fuzzy controllers can operate in a discrete time basis facilitates its integration within existing industrial process control systems [26].

Fig. 1 shows the block diagram of the PID-like fuzzy pH-controller used in this work. According to that, the methodology applied to design the controller has the following scheme to account for the different operations of the controller: (i) input and output variables definition; (ii) scaling factors and membership function; (iii) fuzzy rules formulation; (iv) defuzzification procedure.

2.1. Input and output variables

The pH value measured by the acquisition system was used as an input variable in the control system (Fig. 1). Subsequently, in order to use a PID scheme, the P, D and I terms that will act as the control variables are: the error signal, e; the change of error, Δe; and the sum of errors (integral error), Σe; which are given in the discrete form respectively by:

$$\begin{aligned} e_t &= pH_{sp,t} - pH_t \\ \Delta e_t &= e_t - e_{t-1} \\ \sum e_t &= \left(\frac{1}{2}\Delta e_t + e_t\right) + \sum e_{t-1} = \sum E + e_t \end{aligned} \tag{1}$$

Where the subscript, t, accounts for the present time value of the corresponding variable and $pH_{sp,t}$ refers to the current set point pH value. It is worth to mention that the error value finally used by the fuzzy controller result from multiply equation 1 by −1, as a result the error curve follows the same trend than the pH value and it facilitates the heuristic fuzzy rule formulation.

Analogously with conventional PID controllers, the output is constructed by summing the different actions shown in Eq. (1). It is worth to revise the different information provided by the P, D and I terms. Consequently, the error signal, e, is a direct measure of the difference between the desired output, $pH_{sp,t}$, and the current output pH_t. The derivative term accounts for the trend of the input variable, accordingly a change of error Δe with a negative sign means that the current pH_t output value has increased when

Table 1
Detail of the acidic aqueous solutions used during the runs.

Concentration (mol/L)						
Solutions	Acetic acid	Propionic acid	Strong sulfuric acid	Sodium acetate	Sodium sulfate	Sodium carbonate
S0	0.05	0.025	0	0	0	0
S1	0.004	0	0.004	0.004	0.002	0.001
S2	0.005	0	0	0.005	0.0025	0.00125
S3	0.004	0	0.002	0.004	0.002	0.001
S4	0.01	0	0.01	0	0	0
S5	0.004	0	0.004	0.002	0.001	0.0005
S6	0	0	0.005	0.005	0.0025	0.00125

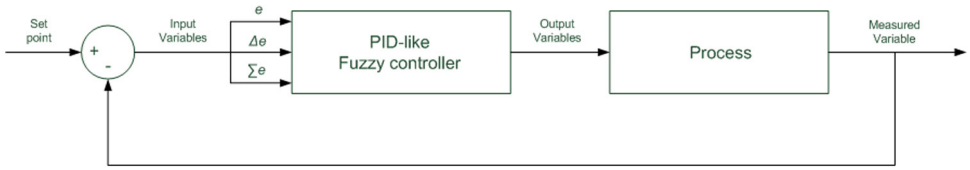

Fig. 1. Block diagram of the PID-like fuzzy control system.

compared with its previous pH_{t-1} value. The integral error component tells about the history of the system.

2.2. The membership functions

With regard to the type of the membership function, a combination of triangular and trapezoidal-shaped element is selected. The trapezoidal-shaped functions are located at the extreme, where no high sensitivity is required, whereas the triangular function occupies the space between the extrema. Such configuration has been broadly applied in fuzzy logic control problems [21,24]. The number of fuzzy sets is related to the sensitivity required by the control action and depends on the characteristic of the system under study, therefore, factors such as the size, type and duration of the pH disturbance, as well as those circumstances related to valve response dynamics and sensitivity will affect the final number of fuzzy sets to be used. In this work the fuzzy controller designed should operate with different acidic aqueous solutions exhibiting buffering conditions (Table 1). Due that the main feature of the fuzzy schemes is that a data point might belong simultaneously to more than one cluster, the choice of the membership structure uses a fuzzy clustering algorithm to estimate the number of fuzzy sets and their location in the data set.

The method finds the number of clusters that best fits the surrogate 'pH data', and it is based on calculating a measure of potential derived from the square distance of the data points to the nearest cluster center [27]. During the potential estimation it is assumed that the influence of a neighboring data point decays exponentially with the square of the distance as follows:

$$P_i = \sum_{j=1}^{n} e^{-\alpha \left\| x_i - x_j \right\|^2} \tag{2}$$

where α is given as:

$$\alpha = \frac{4}{r_a^2} \tag{3}$$

r_a is a positive constant that measures the neighborhood around the cluster center to be evaluated. According to Eq. (3), the method needs the neighborhood ratio to compute the potential. Moreover, to properly select the number of fuzzy sets characterizing the different membership functions it would be necessary to know the hypothetical temporal evolution that the pH value might exhibit as a function of the dimensionless concentration ratio of sodium hydroxide in an open loop situation. When time series of experimental pH data for open loop situations are not available, it is still possible to study the dynamical behavior of the pH value as a function of the dimensionless feeding concentration ratio of sodium hydroxide from the titration curves (Fig. 2).

The titration curve is nothing but a state space plot of the neutralization process, where the pH and the dimensionless sodium hydroxide concentration ratio are the variables used to specify the state of the neutralization process. Accordingly, the titration curves account for the hypothetical complete set of all possible states that the neutralization system can ever be in. As it is well known, for any complex system the major objective is to characterize the underlying process by using the fewest possible number of variables. As stated above, for the proposed PID-like fuzzy pH control system, the variables chosen to describe the system evolution are the control variables (e, Δe, and Σe), consequently as for the titration curve shown in Fig. 2, it is critical to explore the behavior of the control variables in a state space context. Furthermore, both fuzzification and defuzzification operation needs to normalize the control variables applying the standard range of [−1, +1]. The normalization is performed by multiplying each control variable by the inverse of the corresponding maximum expected value. In the case of the error variable the maximum expected depends on the corresponding set point, which in the present work has been set to $pH_{sp,t} = 7$, consequently since the pH value might be in the range between $0 < pH < 14$, the maximum expected error value can be ±7.

Once the error variable has been normalized within the [−1, +1] range, a question arises regarding how to estimate the limit for the change of error, Δe, and the sum of errors, Σe, since those variables are unknown a priory. Nevertheless, both the Δe and the Σe variables are related with the error variable through the expression appearing in Eq. (1), therefore, they could be calculated from a "dynamical" evolution of the normalized error function, e. However, though the state space portrait shown in Fig. 2 reflects the possible movement or evolution of the neutralization system it does not provide any information regarding the underlying dynamics needed to compute either the Δe or the Σe terms. Consequently, it is assumed a random fluctuation behavior of the pH data around the equivalence point pH = 7 to construct a "surrogate" time series of the error function containing all the pH titration curves (Fig. 3a). Later, the corresponding Δe, and Σe surrogates time series are obtained evaluating the expression appearing in Eq. (1) at $pH_{sp,t} = 7$ (Fig. 3b and c). It is worth to point out that in order to design the membership function of the integral action only the fluctuating part of the sum of errors term, ΣE (Eq. (1)), is used. Thus, the subsequent normalization for the Δe and ΣE terms is carried out dividing by the maximum value characterizing the corresponding surrogate time series.

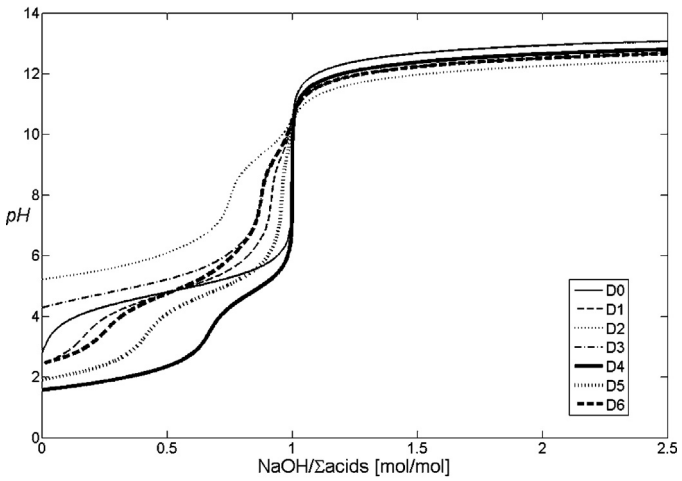

Fig. 2. Theoretical titration curves for the different acidic aqueous solutions used during the runs.

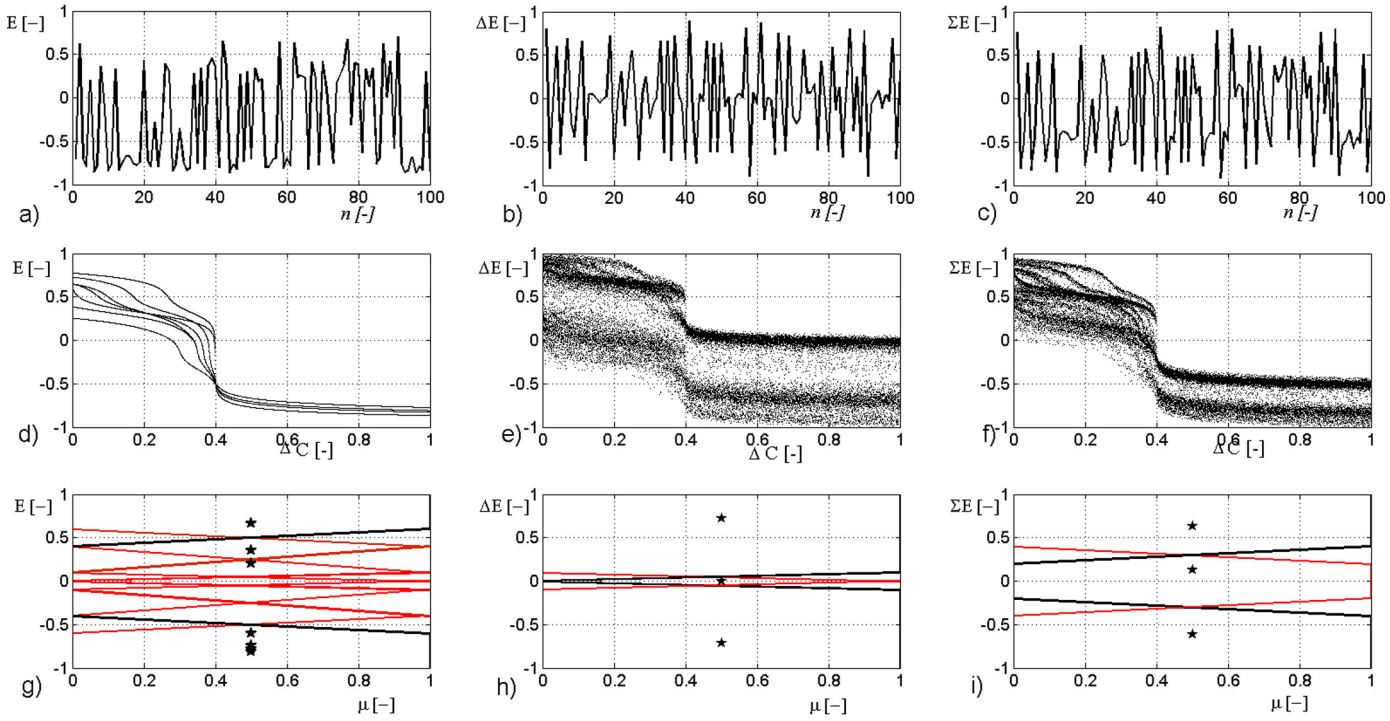

Fig. 3. (a)–(c) Surrogate time series; (d)–(f) State space plots; (g)–(i) Membership functions and cluster center positions from the fuzzy c-means clustering method.

In order to study the performance of the control variables in a state space context, Fig. 3d–f shows a state space representation of the e, Δe, and ΣE terms as a function of the dimensionless normalized sodium hydroxide concentration ratio. It can be observed that the information provided by the error state space plot (Fig. 3d) is analogous to the titration pH curve (Fig. 2), consequently the state space trajectories are well defined and the different titration curves characterizing the solutions shown in Table 1 can be clearly distinguished. In contrast, the trajectories appearing in the state space portraits corresponding to the change of error and the sum of error functions are characterized by points that spread over a wide region of the state diagram (Fig. 3e and f). Moreover, in spite of it some operational windows can be distinguished, (gap regions between operational trajectories) it cannot be identified whether a trajectory point corresponds to a certain titration curve, therefore no information can be extracted on existing buffering conditions. Additionally, it is worth to remark that the state space portraits shown in Fig. 3d–f are noiseless, consequently for current noise experimental time series the resulting state space plots will appear blurred. In this line, the Δe, and ΣE portraits will be more affected by noise that the error function, due that it is expected that noise will make to disappear the gap regions appearing in Fig. 3e and f. Moreover, the dense regions (zones of high popularity on the state space) which are more likely to be visited during the dynamical evolution of the neutralization process will fade out within the data noise.

In order to define the structure of the membership function that account for the P, D and I terms, it is necessary to identify the normalized dimensionless variables that will contribute to the different control actions. As discussed previously, the combined information of the error function (Fig. 3d) and the dimensionless normalized sodium hydroxide concentration ratio provide enough information to specify the state of the neutralization process, making possible to distinguish even between the distinct buffering conditions that characterizes the different acidic aqueous solutions used (Table 1). Therefore, both the error function and the normalized sodium hydroxide concentration ratio constitute a two coordinate trajectory matrix, $x = [\Delta C\ E]$, for the neutralization process, and consequently, such two column vector is used to estimate the number of sets characterizing the structure of the membership function of the P action (the final P actions will use just the error function). With regard to the D and I controller actions (Fig. 3e and f), the state space information provided indicates that, in contrast to the error function state space plot, the complementary use of the normalized sodium hydroxide concentration ratio does not improve the information given separately by either the ΔE and ΣE functions, since for those control variables it is not possible to distinguish the buffer conditions. Moreover, factors such as the noise influence accompanying the measurement which result in a deterioration of the information appearing in Fig. 3e and f makes the change of error and the sum of errors surrogate signals suffice to define respectively the derivative and integral actions. According to that, the ΔE and ΣE functions are used separately as single coordinate trajectory matrix, $x = [\Delta E]$ and $x = [\Sigma E]$, in the fuzzy clustering method to estimate respectively the number of sets characterizing the structure of the membership function of the D and I actions.

Table 2 shows the result from the fuzzy clustering algorithm. It can be observed that according to the potential approach, the minimum number of fuzzy sets needed to describe the proportional, derivative and integral actions are respectively: 6, 3, and 2. The mean absolute deviation, σ_{abs}, has been used as neighborhood ratio in Eq. (3). However, as the Mamdani-type fuzzy processing has been adopted to control the neutralization process, the fuzzy conditional statement needed to calculate a control action are more easily defined for an odd number of fuzzy sets (in order to account

Table 2
Fuzzy sets used to define the membership functions. The first row accounts for the number of sets estimated by the clustering algorithm. The second row defines the final structure of the membership function used in the model.

	Trajectory matrix, [x]	[ΔC E], P	[ΣE], I	[ΔE], D
Fuzzy sets	Clustering algorithm output	6	2	3
	Membership function structure	7	3	3

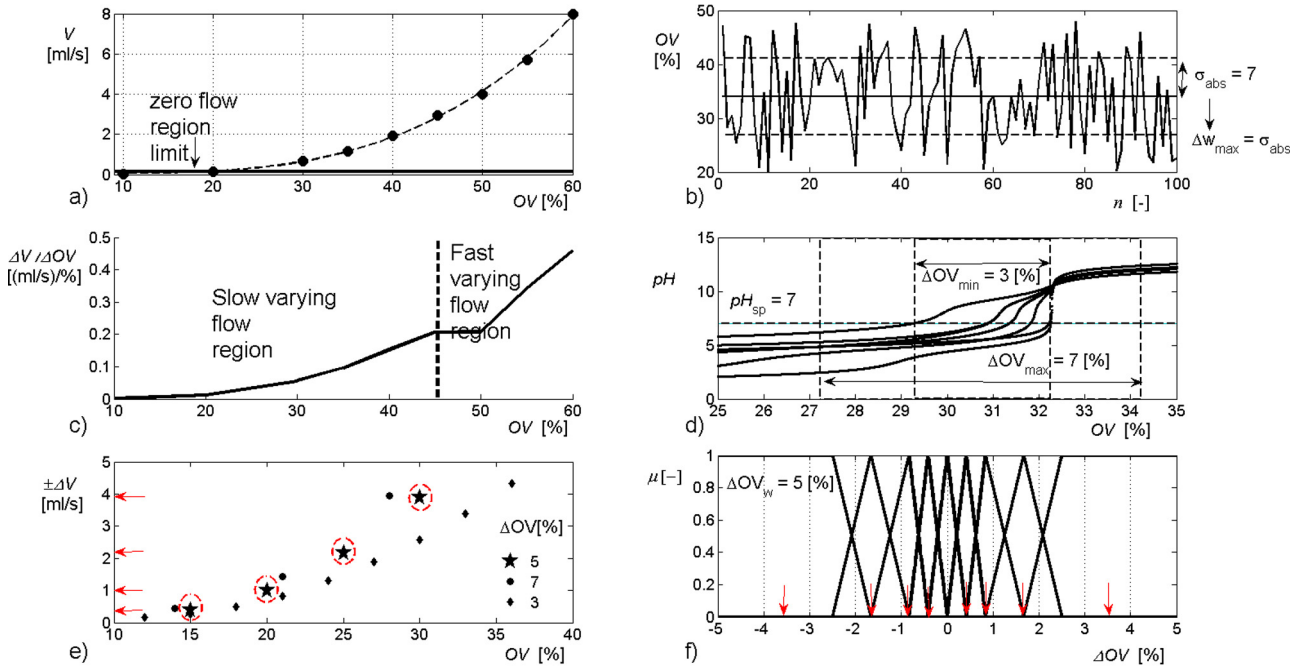

Fig. 4. (a) Experimental valve calibration curve, the dot line correspond to a 3rd degree polynomial fit; (b) surrogate of the percentage valve opening within the normal operation range 20% < %OV < 80%; (c) derivative of the experimental curve calibration data ($\Delta V/\Delta OV$); (d) maximum, ΔOV_{max}, minimum, ΔOV_{min}, and average, ΔOV_w, window size needed to defuzzify the controller output centered over the equivalent region; (e) flow increments on the sodium hydroxide stream due to different maximum step-changes of valve openings ΔOV = 4%(dot), ΔOV = 5%(stars), ΔOV = 6% (squares); (f) membership function and classes for a maximum step change of 5%.

for the "zero condition"). Therefore, the minimum number of fuzzy rules is rounded to the large nearest odd number, consequently the number of fuzzy set to be used finally is fixed to 7, 3, and 3 respectively for the *P*, *D*, *I* actions (Table 2).

With regard to the membership function width there is some agreement in the way that the membership functions describing different sets should overlap: however, what it is not clear yet is the degree of overlapping and consequently, the final membership function distribution choice remains as the major inconvenient found in fuzzy controller design and should be addressed by heuristics. Fortunately, the LabVIEW® software design packages used in this study facilitates the way to define the membership function. Nevertheless, to guide the design the cluster centers characterizing the final membership structure, the fuzzy c-means clustering (*fcm*) algorithm is applied over the *e*, Δe, and ΣE functions by setting the number of cluster used respectively to 7, 3, and 3 [28]. Fig. 3g–i shows the final fuzzy set structures characterizing the membership function of the *P*, *D*, *I* actions. According to that, the *P* and *D* terms are made of triangular and trapezoidal elements, whereas the integral term is composed of trapezoidal elements. The black stars shown on the plots accounts for the *e*, Δe, and ΣE cluster center coordinates estimated through the *fcm* algorithm (Please note that the *fcm* algorithm gives the dimensionless coordinate within the standard range of [−1, +1], consequently the corresponding degree of membership, μ, has been set to zero in Fig. 3 just to center the *fcm* data). The center value of the *e*, Δe, and ΣE terms is used in combination with the corresponding state space plots to arrange the different sets characterizing the membership functions (Fig. 3d–f). For instance, in the case of the error function, the buffer conditions that identify the different acidic solutions used (Table 1) can only be recognized in the upper part of Fig. 3d. According to that the center values of the *e* function corresponding to that region provided by the *fcm* algorithm are well separated, and it can be used to guide the choice of the fuzzy sets. In contrast within the lower region of Fig. 3d, the error coordinate for the different sets would overlap, and they should fall in the same set. Therefore, the upper region information of both error function cluster center and the corresponding state space plot is used to design the triangular elements to be used near the equivalent points, whereas the bottom region is used to size the trapezoidal elements located at the extreme of the membership function.

As for the controller inputs, it is necessary to define the number of fuzzy sets needed to defuzzify the output. Since the controller outputs are step-changes over the percentage of valve opening, a complementary use of the clustering potential algorithm and a study based on the valve rangeability characteristics have been conducted to design the output structure of the fuzzy controller.

The clustering potential algorithm is then used to estimate the order of magnitude of the solution (i.e. number of sets). Accordingly, the coordinates of the trajectory matrix to be used to size the membership function are defined as a function of the variables previously used to design the number of fuzzy sets for the *P*, *I* and *D* actions. Thus, the controller output data matrix used by the fuzzy clustering method read as: $x = [\Delta CE \Sigma E\ \Delta E]$. As a result, the minimum number of sets needed to defuzzify the output should be around 10. According to the methodology followed previously for the control actions, the theoretical minimum number of fuzzy sets should be 11. However, as explained below the maximum number of odd divisions that are finally used was fixed to 9 sets.

In order to study the performance of the control valve, Fig. 4a shows the experimental calibration curve of the control valve used to feed the stream of sodium hydroxide, it can be observed that the maximum valve opening of the control valve is limited to 60%. Besides, the nominal rangeability corresponding to the *D* trim type and equal percentage features reported by Badger Meter inc. is of 50:1.

Prior to decide the number of sets needed to defuzzify the output, it is necessary to size the output range of the change of valve opening, % ΔOV. Consequently, the maximum and minimum controller output range needed to account for the variability of the pH data is estimated. As a result, the final output range used will fall within the region defined among the maximum and minimum

Table 3
Fuzzy sets for integral action value N; Fuzzy sets for integral action value Z, Fuzzy sets for integral action value P.

Integral *N*			Error						
−0.7	Break-points		NB	NM	NS	Z	PS	PM	PB
			−0.6	−0.4	−0.1	0	0.1	0.4	0.6
Derivative	−0.5	*N*	PL	PB	Z	NLL	NL	NL	NL
	0	*Z*	PB	PLL	PLL	NLL	NL	NL	NL
	0.5	*P*	PM	NLL	NM	NL	NL	NL	NL
Integral *Z*			Error						
0	Break-points		NB	NM	NS	Z	PS	PM	PB
			−0.6	−0.4	−0.1	0	0.1	0.4	0.6
Derivative	−0.5	*N*	PL	PB	PM	Z	NL	NL	NL
	0	*Z*	PB	PLL	PLL	Z	NL	NL	NL
	0.5	*P*	PM	NB	NM	NM	NL	NL	NL
Integral *P*			Error						
0.7	Break-points		NB	NM	NS	Z	PS	PM	PB
			−0.6	−0.4	−0.1	0	0.1	0.4	0.6
Derivative	−0.5	*N*	PB	PM	PM	Z	NL	NL	NL
	0	*Z*	PM	PLL	PLL	Z	NL	NL	NL
	0.5	*P*	PLL	PLL	PLL	NL	NL	NL	NL

values. According to that, the maximum controller output range is estimated to size the maximum windows, ΔOV_{max}, that in principle could be used to defuzzify the controller output. To that end, it is assumed that the maximum variability in the pH measured data would correspond to a random variation of valve opening at the current valve operational conditions. According to Fig. 4a the control valve could operate between the maximum flow corresponding to the 60% *OV* and the minimum controllable flow limited by the 50:1 rangeability valve characteristics, such flow of $\Delta V_{min} = 0.16$ mL/s corresponds to a valve opening of 20% *OV* (solid curve). Therefore, since control valves currently operate up to 80% of the maximum valve opening (i.e. 48% *OV*), a surrogate time series of the percentage valve opening within such normal operational range 20% <%*OV* <48% is shown in Fig. 4b. The mean absolute deviation,σ_{abs}, is used to size ΔOV_{max}, and therefore, measures the maximum amplitude change allowed in the controller output, $\pm\Delta OV_{max}$. As Fig. 4b shows, the mean absolute deviation takes a value of $\sigma_{abs} = 7\%$, which corresponds to a maximum step change of $\Delta OV_{max} = \pm 7\%$. After the estimation of the maximum window size, the minimum controller output range, ΔOV_{min}, needed to account for the variability of the pH data is estimated as the width of the equivalent region defined by the titration curve used through the research. It can be observed in Fig. 4d that the ΔOV_{min} equals 3 percentage units. As shown below, the final size of the output range of the change of valve opening was chosen as the mean value between the maximum and minimum extreme as: $\Delta OV_w = \pm 5\%$, being therefore the maximum amplitude change allowed in the controller output.

Furthermore, through the design process, it has been taken into account the point that equal percentage control valves are characterized by the fact that equal increments in valve position result in equal percentage increments in the exiting flow, regardless of the existing flow. Therefore, the same step-change results on a different sodium hydroxide stream flow depending on the current valve opening value. According to that Fig. 4c shows the derivative of the experimental calibration curve (Fig. 4a). As a result, it can be clearly distinguished a slow varying flow region (on the lower part of the calibration curve), and a fast varying flow region (corresponding to the upper part of the calibration curve).

Consequently, in order to estimate the number of fuzzy sets needed to defuzzify the output by using a Mamdani-type fuzzy processing, the flow increments, ΔV, obtained at different step changes, ΔOV, of 7%, 3%, and 5%, over the whole range of valve opening operational conditions was explored (Fig. 4e). Those step changes correspond respectively with the maximum and minimum windows sizes, and with the mean window size finally used to set the controller output. Thus, Fig. 4e gives a picture of the control valve response against different maximum step-changes of valve openings, $\pm\Delta OV$. According to the equal percentage characteristic of the control valve, a direct analogy is established among ΔV and ΔOV, in the way that the maximum step change allowed in the valve opening is expected to be in the controlled flow. According to that, in Fig. 4e the number of points above the zero flow region gives the valve position (i.e. number of sets) needed to operate the control valve within the amplitude change defined respectively by ΔOV_{max}, ΔOV_{min}, and ΔOV_w step changes. In consequence, the step change of $\Delta OV_{max} = 7\%$ results on three points above the zero flow region. Therefore, the corresponding membership function has 7 sets, 6 to deal with $\pm\Delta OV$ step changes, and 1 additional class to manage the zero flow region condition. In accordance, the step change of $\Delta OV_w = 5\%$ presents 4 points above the minimum controllable flow region and consequently, its membership function has 9 sets; 8 to deal with $\pm\Delta OV_w$ step changes, and 1 additional set to manage the zero flow region condition (Fig. 4f), and so on for the $\Delta OV_{min} = 3\%$ which would lead to 19 sets.

In one hand, as a result of the clustering potential algorithm estimate, the minimum number of fuzzy sets needed to defuzzify the output should be around 11. On the other hand, from the analysis of the maximum step change it seems that 7, 9 or 19 sets might serve to provide a reliable valve control within the slow, fast and zero flow regions (Fig. 4c). Then some tricky question arises about what is the right choice? Unfortunately, the question should be answered through practice. Hence, since from a Mamdani-type fuzzy rule processing the number of fuzzy rules needed to perform the control action depends on the number of sets, the less elements the simpler the control action, initially the output membership function was defined having 7 sets. However, the resulting fuzzy controller performance was rather unsatisfactory due to the appearance of unwanted offset and overshooting problems, and slow reaction rates. Therefore, the next Mamdani-type fuzzy rule configuration having 9 sets was used, such value is close to the number of fuzzy sets estimated previously through the clustering algorithm, and correspond to a valve operational region within a $\Delta OV_w = \pm 5\%$ maximum step change. As it is shown through the paper such membership structure provides a reliable pH control for

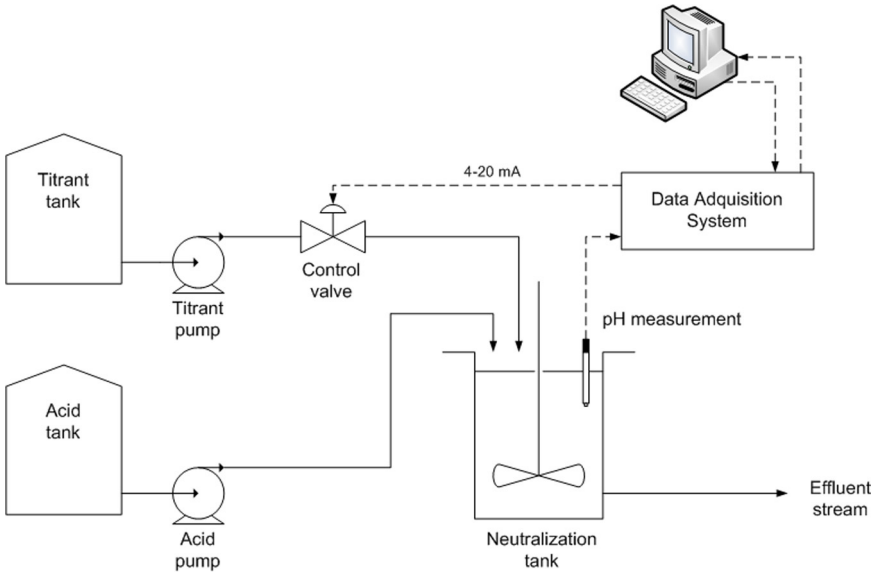

Fig. 5. Experimental set up.

the operational PL conditions covered. The use of the next configuration corresponding to 19 classes would make even more difficult the subsequent rule formulation.

Moreover, thanks to the analogy between ΔV and ΔOV, the ordinate coordinate axis of the points above the zero flow region (stars of Fig. 4e) can be used as a first estimate of the center of the triangular and trapezoidal elements that constitute the membership function (arrows of Fig. 4e and f).

2.3. The fuzzy rule formulation

Heuristics is needed to derive the fuzzy control rules, thus the high sensitivity to small perturbations of $[H^+]$ that the titration curves exhibit close to the equivalence point (Fig. 2) is taken into account to guide the fuzzy rule formulation. Since the controller input defined by the *P*, *I*, and *D* actions derived above has respectively 7, 3, and 3 conditions, the number of fuzzy rules needed is $N_{fR} = 7 \times 3 \times 3 = 63$, which are shown in Table 3. According to that the conditions for error function are: Negative Big, NB, Negative Medium, NM, Negative Small, NS, Zero, Z, Positive Small, PS, Positive Medium, PM, Positive Big, PB. Whereas for the derivative and integral actions are: Positive, *P*, Zero, *Z* and Negative, *N*. The final break point used for the membership functions are also given.

As depicted in Table 3, the conditions for the valve aperture are: Positive Large, PL, Positive Big, PB, Positive Medium, PM, Positive Little, PLL, Zero, Z, Negative Little, NLL, Negative Medium, NM, Negative Big, NB, and Negative Large, NL.

The heuristic process of fuzzy rule formulation has two steps: during the first step the 63 rules are approximated with the help of a model of a conventional PID controller. Later, through the second step the fuzzy rules are optimized heuristically according to the experimental observations and the data collected during the experimental runs about the rules utilization, such information is provided by the LabVIEW® software. The model provides case studies for the heuristic definition of the fuzzy rules before the experimental optimization. An example of the derivation of the first approximation of the fuzzy rules is presented in Appendix B.

2.4. The defuzzification procedure

The center of maximum method (CoM) is applied to produce the output of the Mamdani PID-like fuzzy controller developed in this work. Accordingly the fuzzy logic controller first compute the mean of the numerical values corresponding to the degree of membership of the different fuzzy sets and later the outputs of the of the *P*, *D* and *I* actions are averaged taking into account the current values at which the membership function were scaled. The CoM in discrete form read as:

$$y = \frac{\sum_{i=1}^{k} u_i \mu_i}{\sum_{i=1}^{k} \mu_i} \tag{4}$$

where u_i is the typical numerical value for the scaled membership function *i*, and μ_n is the degree of membership at which membership function *i* was scaled (*k* accounts for the membership functions averaged).

3. Experimental

To test the performance of the PID-like fuzzy controller, both simulate and experimental runs of different acidic aqueous solutions exhibiting buffering conditions consisting on acetic and propionic acids were neutralized in a single CSTR with sodium hydroxide having a molar concentration of [NaOH] = 0.2 mol/L. In order to produce buffering conditions, the acidic stream can also include sulfuric acid and common ion salts such as sodium acetate, sodium carbonate and sodium sulfate (Table 1). The equilibrium reactions considered during the simulation runs as well as the theoretical model of the neutralization process used to test the controller have been included in Appendix A.

3.1. Experimental set-up

The experimental setup used in this research consist of a continuous stirred tank having a volume of $V = 1.75$ L. The mean residence time value, V/Q, of the liquid solution ranges between $5 < t_r = V/Q < 30$ min, and the effluent weir located at the vessel side keep the level fairly constant during the neutralization process (Fig. 5). The runs were carried out at room temperature (around 25 °C) and during the steady state operation the feeding concentrations were those corresponding to the *S0* solution (Table 1). The feeding flow rate of the acidic stream in steady state is $3 \times 10^{-3} L/s$ (Fig. 4), and the sodium hydroxide used as a titrant agent has a molar concentration of [NaOH] = 0.2 mol/L. The pH electrode is an

Ag-AgCl electrode with internal reference, saturated with a 4 M KCl solution. During the experimental runs, the electrode was placed in the tank as shown in Fig. 5. As it is described in Fig. 5, the feedback PID-like fuzzy control loop is based on a distributed I/O hardware provided by NATIONAL INSTRUMENTS®, where a FP1000 controller interface connected to a FP-TB-10 terminal base is configured with FP-AI-V10 analog input and FP-AO-C420 output modules. Accordingly, a CRISON pH-Meter GLP 21 provides the measured pH voltage signal, which is digitized through the dual-channel voltage module at a sampling rate of 1 s, whereas the current output that accounts for the control actions is sent as a 1–20 mA output signal to a I/P, ITT 40 mA, 3–15 psi converter fitted to a pneumatic control valve (Badger Meter, Inc., model D-Research, ATO, equal percentage trim, coefficient 0.8). The maximum valve opening usable for control purposes is 60%. The acquisition system was connected to a computer by means of a RS232 port. The computer code used for monitoring and controlling the neutralization process was implemented in LabVIEW®.

4. Results and discussion

In this work, the neutralization process is treated as regulatory control problem, where the controlled pH value might deviates from set point because of disturbances. Therefore, the feedback PID-like fuzzy control system designed should compensate those disturbances. According to that, the experimental procedure assumed either during the simulations runs and in the experimental study suppose that the system is operating at steady state conditions, consequently the run is initiated in open loop configuration by using the *S0* solution as the nominal case (Table 1). Subsequently, the control loop is closed and a set point of $pH_{sp,t} = 7$ is established to leave the fuzzy controller to guide the process to get the steady state operational conditions.

The dynamic analysis of the transient response to step-change perturbations is conducted to test the controller performance. As shown in Table 4, the variables used to induce the step-change disturbances are respectively: (i) the acetic and propionic acidic flow rates; (ii) the propionic acid concentration; (iii) acidic stream substitution. Accordingly, the step-change perturbations, $\Delta C(\%)$, regarding both the acetic and propionic acidic flow rates, and the propionic acid concentration were induced either in upwards or downward direction ranging between $\pm 50 < \Delta C(\%) < \pm 200\%$ (Table 4).

The dynamical response against acidic stream substitution tests serves to study the controller performance under different process gains (buffering conditions). The different reaction curves characterizing the transient response of the neutralization process is later described in terms of its effective lag (dead time), reaction rate

Table 4
Step change perturbations used in both simulated and experimental runs and experimental rejection times.

Disturbance loads	Step-change	Rejection time, τ_r,[s]
Acidic flow rates $\Delta Q(\%)$	50	50–120
	70	220
	100	CYCLING
	150	CYCLING
	200	CYCLING
Propionic acid concentration $\Delta C(\%)$	50	75
	100	40
	200	40–180
Acidic stream substitution	D1	100
	D2	100
	D3	180
	D4	180
	D5	80–180
	D6	100–180

$r_{(H)} = 5\tau$, the process reaction time and characteristic time τ (time taken for the process variable, i.e. pH value, to reach 63.2% of its maximum value).

4.1. Simulate runs

The simulation runs were used to verify the stability and performance of the structure of the feedback PID-like fuzzy controller designed above. Fig. 6 shows the closed-loop step of the start-up operation for both simulate and experimental runs. It is worth to mention the remarkable matching between simulated and experimental pH data, the reaction curves for both cases almost match (Fig. 6a), being the characteristic time, $\tau \sim 220$ s, and the reaction rate, $r_{(H)} \sim 1000$ s, almost equal. The small differences observed are attributed to the dead time existing in experimental time series, the control valve, and signal noise. Fig. 6b shows the comparison between simulated and experimental percentage of valve opening, as for the pH curves, the behavior of the experimental valve follows the controller output predicted by the model, only small differences in the line-out portion of the curve due to valve rangeability are observed. Finally, the *P*, *I*, and *D* actions also match those for the simulated runs. The little differences observed are explained by the measurement noise characterizing the current measured pH signals.

Since a tight control over the pH value is required, the desired transient response of the control system should exhibit no overshoot. Thus as shown in Fig. 6, the PID-like fuzzy controller designed fulfills the non-overshoot condition and therefore, the dynamic analysis of the transient response to step-change perturbations is conducted below to test the expected controller performance.

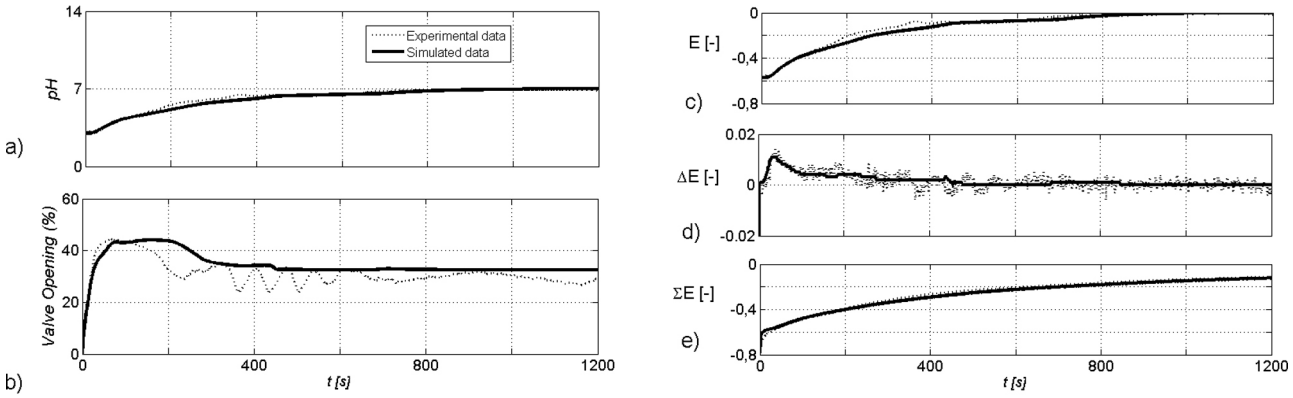

Fig. 6. Model vs. Experimental during start-up operation of: (a) pH variable; (b) percentage of valve opening; (c) *E* term; (d) ΔE term; (e) ΣE term.

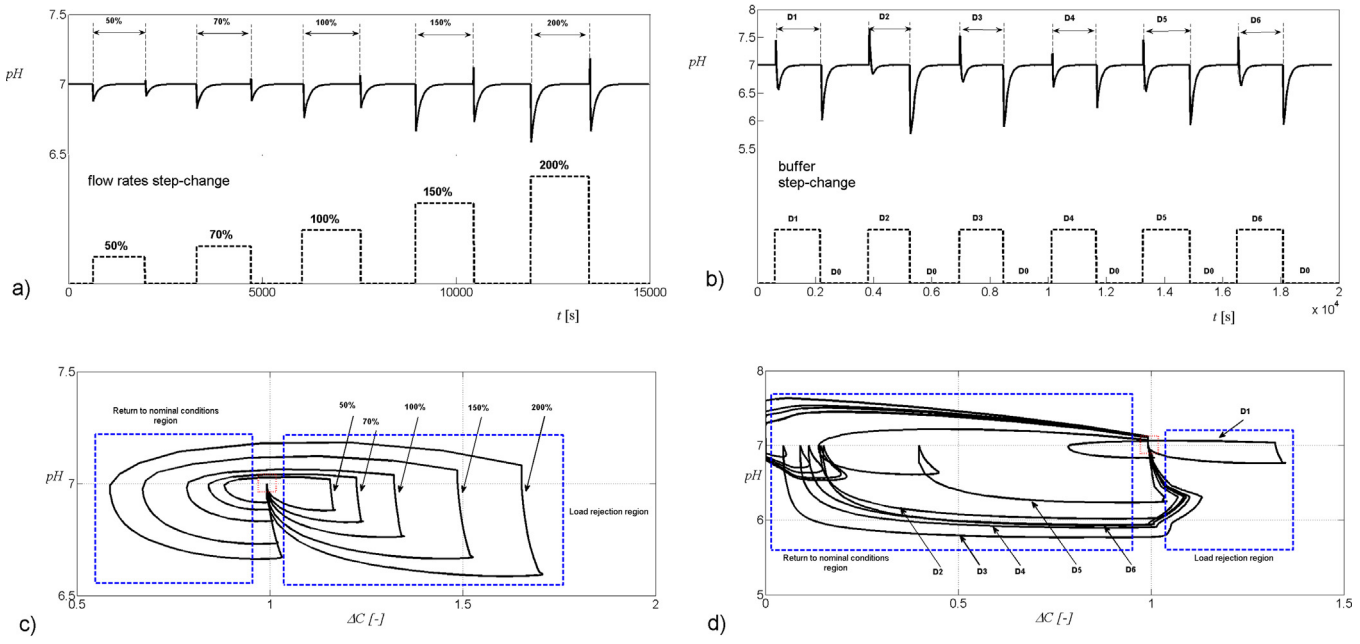

Fig. 7. Simulated pH time series for step-change perturbations of: (a) propionic acidic flow rates; (b) acidic stream substitution (c) State space plot of the propionic acidic flow rates perturbation; (d) State space plot of the acidic stream substitution.

According to that, Fig. 7a and b presents respectively the response of the controller against changes of the propionic acidic flow rates, and acidic stream substitution. In Fig. 7a and c it can be observed that the different step-change perturbations are rejected in timely manner, being the characteristic time for change rejection of the same order of the dead time characterizing the pH measurement (Fig. 6a). Moreover, it has been observed that the changes either of the propionic acidic flow rates or of the propionic acid concentration are rejected by the fuzzy controller without succeeding overshooting and with a minimum deviation from the set point value. Furthermore, the acidic stream substitution step-change produces a neutralization process characterized by a different gain (i.e. buffering conditions) result in a larger deviation from the set point of the pH value. The transient response changes because the process gain is defined by the new acidic solutions used (Fig. 7b). As for the state space plots, Fig. 7c shows how for the *S0* solution the simulation runs predict a tight control around the set point, consequently it can be observed how the large trajectories corresponding with the larger perturbation are confined within a narrow region around the set point within the state space. For the acidic stream substitution case, Fig. 7d shows a wider operational region needed by the controller to recover the nominal operational conditions. Furthermore, it can be observed that the response of the neutralization process against flow and acidic stream substitution is clearly different. The differences observed between Fig. 7c and d are attributed to the changing gain conditions of the acidic stream substitution runs.

4.2. Experimental runs

Once the fuzzy controller has been optimized for the simulation data, acidic flow rates, propionic acid concentration and acidic stream substitution disturbances were induced to test the controller performance through experimental runs. Statistical analysis was used to evaluate the controller performance. Accordingly, the variations due to the step-changes studied below are discussed to verify if the process is running satisfactorily. Namely, it is assumed that the current pH measured data will follow a normal distribution and it is expected that more than 99 per cent of the pH samples should lie between the lines marked as the Upper Action, *UA*, and the Lower Action, *LA*. These action lines are set at a distance equal to $\overline{\mathrm{pH}}_n \pm 3\sigma$ around the stationary mean value, $\overline{\mathrm{pH}}_m$. Thus, for stationary operational conditions, the likelihood of a point falling outside either of these lines should be close to 1 in 1000, unless some 'unexpected' load modifies the process during the sampling interval.

Fig. 8a shows the *UA* and *LA* limits as well as the warning limits the *UWL* and *LWL* lines statistically set as: $\overline{\mathrm{pH}}_n \pm 2\sigma$. The pH data

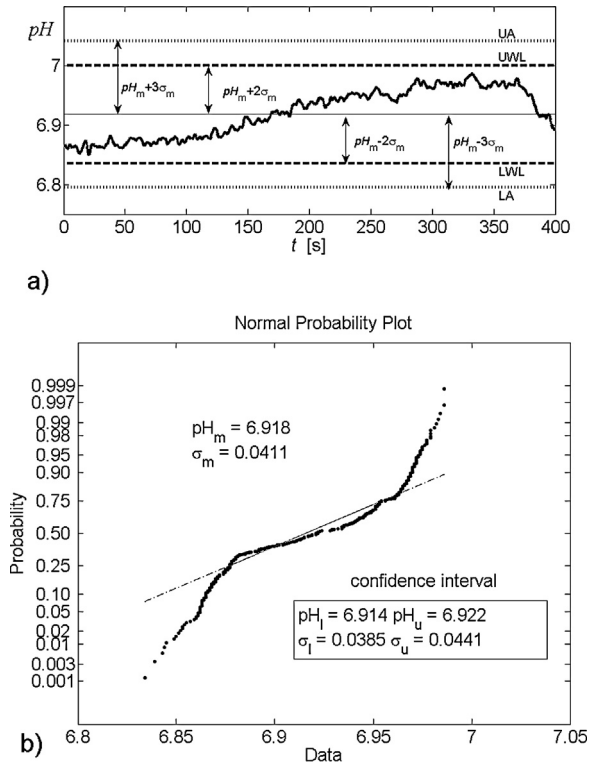

Fig. 8. (a) Experimental pH time series corresponding to the stationary steady state operation; (b) Normal probability plot function.

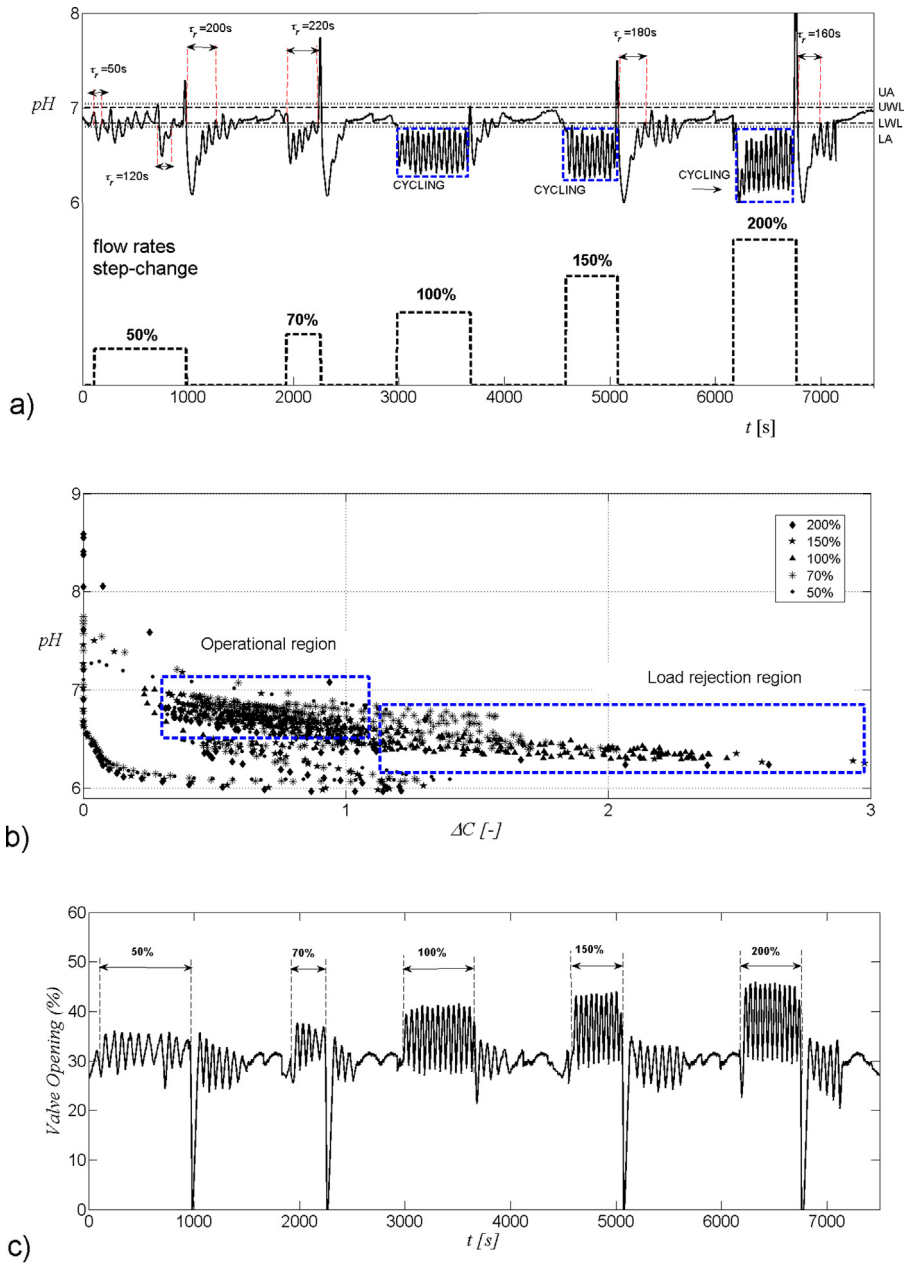

Fig. 9. Measured pH time series for step-change perturbations of propionic acidic flow rates: (a) pH time series data; (b) state space plot; (c) % Valve opening.

falling in the region within the upper and lower limits are assumed to be satisfactory, and consequently no control action should be required for those operating conditions. Moreover, Fig. 8b presents the corresponding probability mass function for the data used to characterize the stationary state operation. As it can be observed, the experimental distribution of the data (dot line) deviates from a normal distributed plot (dash line). Fig. 8b shows the mean values of the pH and the standard deviation, σ, used to define the *UA*, *LA*, *UWL* and *LWL* control lines, as well as the confidence interval containing the 'true' pH and σ values.

In order to measure quantitatively the performance of the fuzzy controller for load rejection, the '*control lines*' are included in the pH control chart. During the experimental runs the reaction rate, $r_{(H)}$, will be measured in terms of rejection time, τ_r, which measures the time that the current measured pH_t value is located outside either of the *UA* or the *LA* lines. Consequently, τ_r is taken as a measure of the control rate.

4.2.1. Dynamic transient response against flow rates changes

Fig. 9a shows the behavior of the pH measured data against acidic flow step changes, it can be observed how the controller is able to reject flow rates loads of 50% and 75% in a time of the order of the characteristic time, $\tau_r \sim \tau$. However, for large acidic flow rates resulting from the positive load of 100%, 150% and 200%, the controller is unable to make the process to operate satisfactorily within the *UWL* and *LWL* lines. In contrast, as it can be observed in Fig. 9, the controller barely succeed in keeping the process operating intermittently in the region defined between the *UWL* and *LA* control lines. The reason of the cycling behavior is attributed to a reticulating signal produced as a consequence of the large acidic flow rate, the reactor do not longer behaves as a perfectly stirred reactor and consequently, the acidic disturbance by-pass the reactor and enter the control loop as a 'slug', which result on a control action that reverses the direction of the signal by opening the control valve. At the end of the dead time, the titrant slug reaches the pH electrode

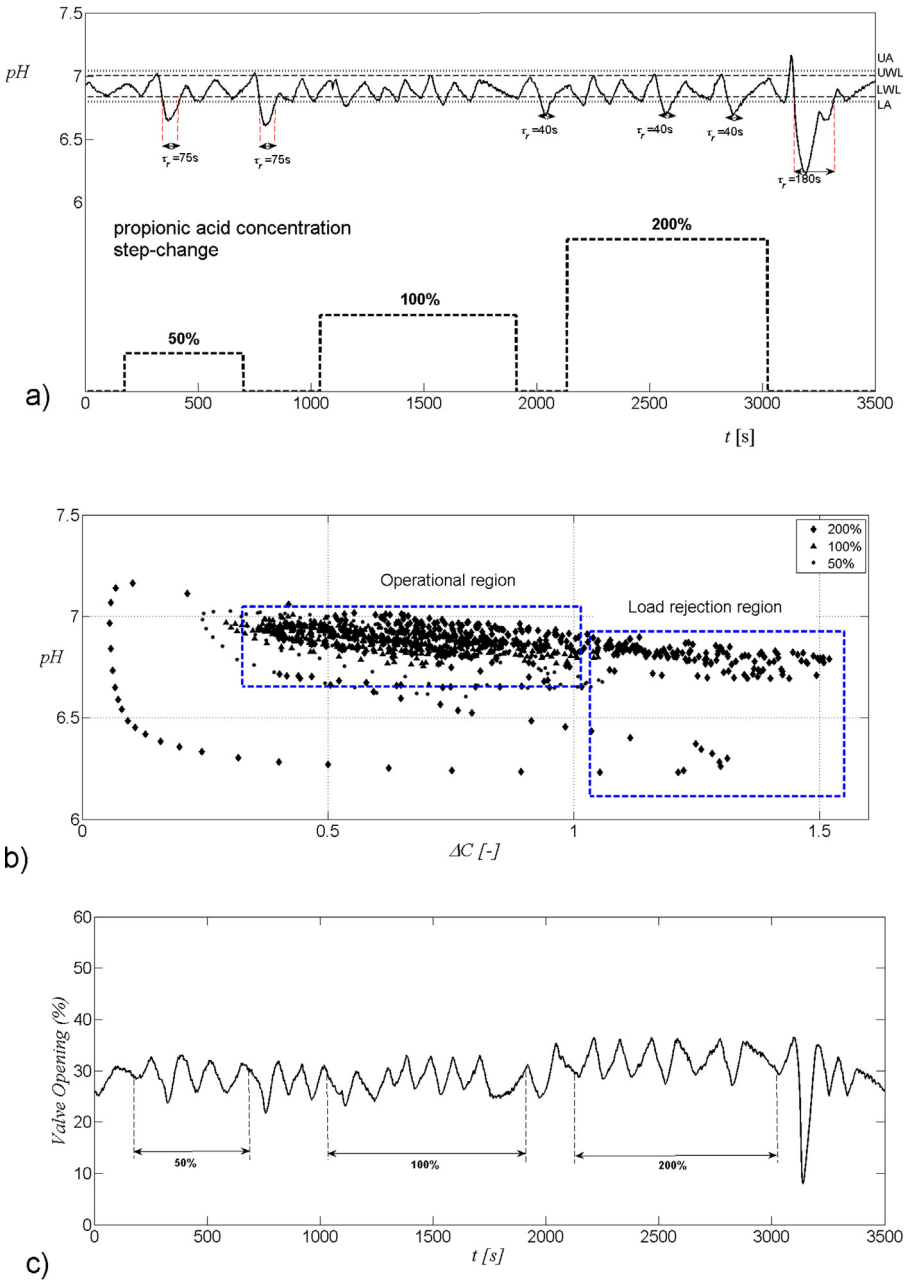

Fig. 10. Measured pH time series for step-change perturbations of the propionic acid concentration: (a) pH time series data; (b) state space plot; (c) % Valve opening.

and the controller corrects the pH decrease by closing the valve. As a result, the control system cannot eliminate the cycling. The effect of such cycling behavior on the valve opening is an undesirable oscillating movement that might result in a premature damage of the control valve (Fig. 9c). Nevertheless, those results are presented here to illustrate the reliability of the controller performance under extreme operational conditions that are not expected to be found in practice in those regulatory control problems.

With regard to the state space plot (Fig. 9b), it can be observed that the effect of the cycling at higher acidic flow rates makes the neutralization process to occur on a wider region that for lower acidic flow rates. Moreover when cycling behavior occurs, the neutralization process is confined within the load rejection region shown in Fig. 9b.

4.2.2. Dynamic transient response against the propionic acid concentration

As shown in Fig. 10, the control loop response against the small disturbance of propionic acid concentration is generally faster than for small disturbances of acidic flow rates step-changes, $\tau_r \sim 75$ s. The fuzzy controller always drives the neutralization process to operate within the *UWL* and *LWL* lines. Moreover, no cycling behavior is observed for large disturbance loads, which result in a more stable operation of the control valve (Fig. 10c). As a result, the state space plot of the transient response against the propionic acid concentration is narrower than for the acidic flow rates step-changes case (Fig. 10b). It can be observed that, in contrast to the flow rate step changes, now the load rejection region is considerably smaller.

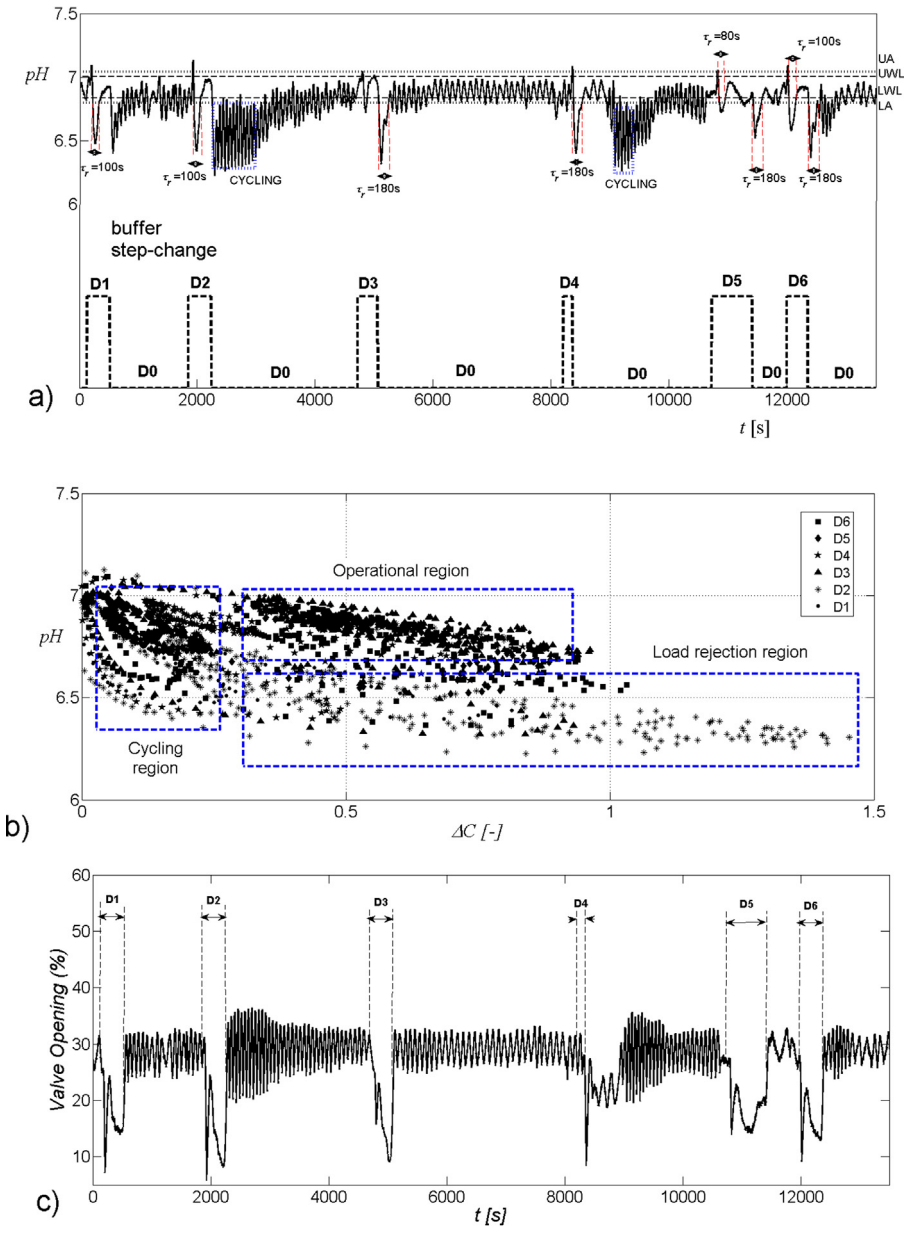

Fig. 11. Measured pH time series for buffer step-change perturbations: (a) pH time series data; (b) state space plot; (c) % Valve opening.

4.2.3. Dynamic transient response due to buffer change conditions

Finally the dynamical response against acidic stream substitution is conducted in order to test the controller performance under different process gains. Fig. 11a shows the measured pH signal for different buffer step-change solutions. It can be observed that in spite of the controller is able to reject the process gain disturbances, the load rejection time is strongly depending on the direction of the load. Accordingly, whereas τ_r is of the same order than the characteristic time, τ, when the nominal buffer solution, *S0*, is replaced by any of the test solution (*S1*–*S6*). The time to recover the initial steady state conditions when the disturbance cease and the system is feeding again with the *S0* solutions, is considerably larger and strongly depends on the mean residence time value of the liquid solution. Thus, as it is observed in Fig. 11a, the mean residence time of the liquid solutions corresponding to the *S2* and *S4* which ranges between 10 min > t_r > 15 min, facilitates the appearance of a recirculating signal (Fig. 11a and c), that might be explained by the arrival to the pH electrode of slug composition traces belonging to the *S2* and *S4* solutions. However in contrast to the previous acidic flow rate changes, once that the traces of the *S2* and *S4* solutions disappear, the controller is able to eliminate the cycling. As a result of the control under non-stationary gain conditions the control valve exhibit a vigorous oscillation as for the cycling conditions observed previously for high flow rates loads.

With regard to the state space analysis, it can be observed in Fig. 11b that the cycling behavior observed when the buffer load is removed is restricted to occupy a certain region of the state space characterized by low dimensionless feeding concentration ratio.

5. Conclusions

The response of the feedback PID-fuzzy controller against large perturbations in buffering acidic liquid streams, acidic flow rates and propionic acid concentration is adequate since it maintains the pH value near the equivalence point of $pH_{sp} = 7$, when the neutralization process is operating near the inflection points of the titration curve of the corresponding acidic medium. The *UA*, *LA*, *UWL*

and *LWL* control lines have been used to measure the controller performance.

The structure of the controller consisting in 63 fuzzy rules succeed in keeping the pH value around the set point pH_{sp} = 7. However, due to the absence of an acid control valve there are 21 rules that are never used by the controller. It has been observed that even for the most unfavorable conditions (large loads on acidic flow rates and buffer acidic liquid stream), the neutralization process takes place in a narrow region having a maximum average deviation of 0.5 pH units from the equivalence point. Therefore it is considered that tight control is achieved for the neutralization conditions covered. However, from the results it is not clear yet why the integral of error actually provides benefit to the controller performance. Moreover, since the membership functions of the fuzzy controller have been designed from a random surrogate of the expected pH values, the fuzzy controller does not need the previous knowledge of the titration curves of the acidic solutions.

The stationary cycling behavior observed for large loads of acidic flow rates is attributed to reticulating signal produced as a consequence of 'slug' flow conditions in the vicinity of the pH electrode. Accordingly, there is an intermittent disturbance between the acidic load and the titrant agent that results in a cycling signal that the controller cannot eliminate. Simultaneous pH measurement at different locations and redundant operation of the pH electrodes might result in an improvement of the control action.

When operating at non-stationary gain conditions, the rejection time has been found strongly dependent on the mean residence time of the liquid solutions that give rise to a transitional cycling behavior of the measured pH signal after which the controller is able to eliminate the cycling and consequently drives the neutralization process near the set point value. Such residence time is closely related to the degree of mixing and therefore, it can be seen as a delay time added to the controller action.

The complementary use of state space analysis with fuzzy clustering algorithms has been found extremely useful to design the structure of the fuzzy controller.

Acknowledgments

The authors would like to thank the financial support from projects DPI2009-10518 (MICINN) and CARDENER-CM (S2009ENE-1660).

Appendix A.

The process used to test the controller performance is the continuous neutralization with an aqueous solution of sodium hydroxide of aqueous solutions of acetic and propionic acids with sodium hydroxide in a single CSTR. Furthermore, in some runs, other solutions are used for acidic stream substitution to provide buffering conditions. The equilibrium reactions taking place in an aqueous mixture of acetic acid, propionic acid, and sodium hydroxide are shown in Table A1.

Table A1
Equilibrium reactions and transient state equations considered during the model simulation.

Equilibrium reactions	Transient state equations
$CH_3CO_2H \leftrightarrow CH_3COO^- + H^+$ $CH_3CH_2CO_2H \leftrightarrow CH_3CH_2COO^- + H^+$	$Q_{\alpha,in}\alpha_{in} - Q_{\alpha,out}\alpha_{out} = V_R \frac{d\alpha}{dt}$
$CO_3Na_2 \rightarrow CO_3^{2-} + 2Na^+$ $H_2CO_3 \rightarrow COH^- + H^+$	$Q_{\beta,in}\beta_{in} - Q_{\beta,out}\beta_{out} = V_R \frac{d\beta}{dt}$
$COH^- \rightarrow CO_3^{2-} + H^+$ $SO_4H_2 \rightarrow SO_4H^- + H^+$	$Q_{\gamma,in}\alpha_{in} - Q_{\gamma,out}\gamma_{out} = V_R \frac{d\gamma}{dt}$
$SO_4H^- \leftrightarrow SO_4^{2-} + H^+$ $SO_4Na_2^- \rightarrow SO_4^{2-} + 2Na^+$	$Q_{\delta,in}\alpha_{in} - Q_{\delta,out}\alpha_{out} = V_R \frac{d\delta}{dt}$
$CH_3CO_2Na \leftrightarrow CH_3COO^- + Na^+$ $H_2O \leftrightarrow H^+ + OH^-$	$Q_{\varphi,in}\alpha_{in} - Q_{\varphi,out}\alpha_{out} = V_R \frac{d\varphi}{dt}$

The theoretical model of the neutralization process for numerical simulation purposes is later obtained by solving the charge and material balances expressed in the function of the process invariants such as the dissociation constants K_a, K_p, K_1, K_2, and K_S, characterizing the acetic, propionic, bi-carbonic, carbonic, and sulfuric acids which provide the buffering conditions, and the corresponding water dissociation constant, K_W. Subsequently, the pH of the reacting mixture, assuming a dilute ideal solution at 25 °C, is calculated from the following charge balance equation:

$$\left(\frac{\alpha}{1+\frac{[H^+]}{K_A}}\right) + \left(\frac{\beta}{1+\frac{[H^+]}{K_p}}\right) + \left(\frac{\delta K_1}{1+\frac{K_1}{(H^+)}+\frac{K_1K_2}{(H^+)^2}}\right)\left(\frac{1}{(H^+)}\right)\left(\frac{2K_2}{(H^+)}+1\right) + \phi\left(\frac{(H^+)+2K_S}{(H^+)+K_S}\right) + \left(\frac{K_W}{(H^+)}\right) - \gamma - (H^+) = 0$$

where α, β, γ, δ and φ are the invariants shown in Table A2.

Finally, the concentrations of the different species involved in the equilibrium reaction shown in Table A1 are calculated from a control volume analysis of the invariant components over the CSTR. Such balances are given by the transient state equations appearing in Table A1.

Appendix B.

Fig. A1 shows a possible error response of a simulated conventional PID controller against acidic disturbances, which serves to illustrate the heuristic rules definition process. The error shown in Fig. A1 result from multiply Eq. (1) by (−1), as for the error value finally used by the fuzzy controller, as a result the error curve follows the same trend than the pH value and facilitates the heuristic fuzzy rule formulation.

Accordingly, taking into account the structure of the fuzzy controller, the error chart has been divided into 7 regions corresponding to the fuzzy sets of the "Proportional action". Therefore

Table A2
Equilibrium constant and process invariant considered during the model simulation.

Dissociation constants	Invariants
$K_A = \frac{[CH_3COO^-]\cdot[H^+]}{[CH_3COOH]} = 1.58\cdot10^{-5}$ mol/L	$\alpha = [CH_3COO^-] + [CH_3COOH] = [CH_3COONa]_0 + [CH_3COOH]_0$
$K_p = \frac{[CH_3CH_2COO^-]\times[H^+]}{[CH_3CH_2COOH]} = 1\times10^{-5}$ mol/L	$\beta = [CH_3CH_2COO^-] + [CH_3CH_2COOH] = [CH_3CH_2COOH]_0$
$K_1 = \frac{[CO_3H^-]\cdot[H^+]}{[CO_3H_2]} = 4.45\cdot10^{-7}$ mol/L	$\gamma = [Na^+] = [NaOH] + 2[NaSO_4] + 2[Na_2CO_3] + [CH_3COONa]$
$K_2 = \frac{[CO_3^{2-}]\cdot[H^+]}{[CO_3H^-]} = 4.69\cdot10^{-10}$ mol/L	$\delta = [Na_2CO_3]_0 = [CO_3^{2-}] + [CO_3H^-] + [CO_3H_2]$
$K_S = \frac{[SO_4^{2-}]\cdot[H^+]}{[SO_4H^-]} = 0.013$ mol/L	$\phi = [Na_2SO_4]_0 + [H_2SO_4]_0 = [HSO_4^-] + [SO_4^{2-}]$
$K_W = [H^+]\cdot[OH^-] = 1\cdot10^{-14}$ mol/L	

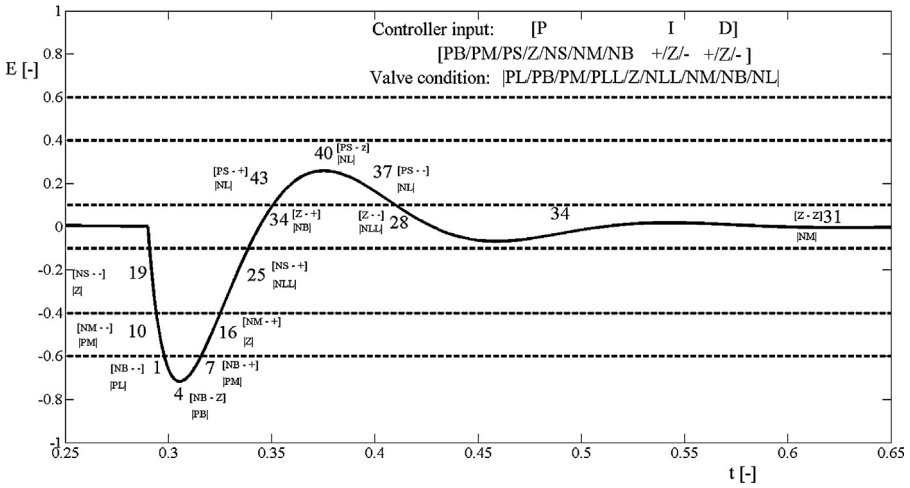

Fig. A1. Response of the analogous PID controller used during the heuristic fuzzy rules definition process.

any error value will fall within some of these chart regions. Consequently, for a certain error value, and a given integral action as positive, *P*, zero, *Z*, or negative, *N*, three rules can be specified by each of the chart regions of Fig. A3. The rules are identified by the three distinct derivatives actions that can characterize the controller input (*P*, *Z*, *N*) for each of the chart regions. Such reasoning provides $3(D) \times 7(P) = 21$ rules for each integral action and therefore, $21 \times 3 = 63$ rules for the PID-like fuzzy controller.

The curve shown in Fig. A1, illustrates the fuzzy rules drawn procedure during the first step of the heuristic process of fuzzy rule formulation. In Fig. A3 the integral action of the analogous PID-like fuzzy controller is assumed to be always negative. The controller inputs are given within brackets whereas valve conditions (i.e. controller output) are given within straight braces. Thus once the controller input has been established according to the membership functions of the controller structure, the corresponding

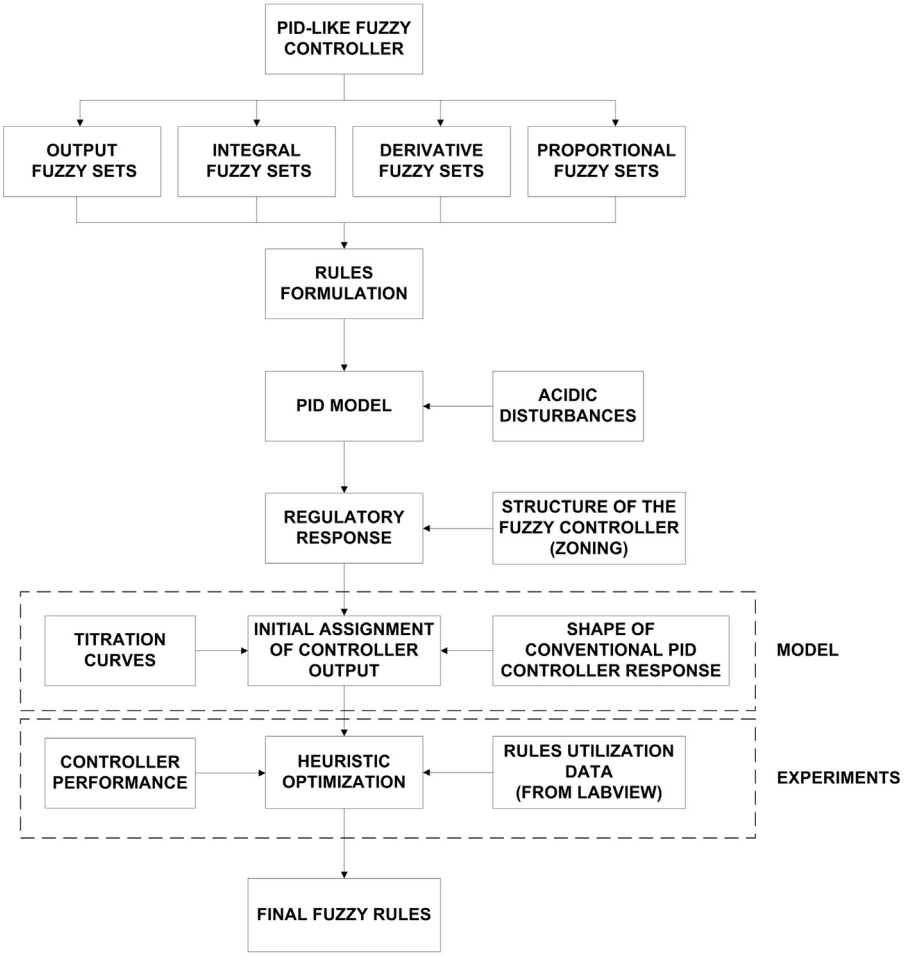

Fig. A2. Tuning procedure scheme.

controller output is assigned by hand taking into account the shape of both the analogous conventional PID controller and the properties of the titration curves near the equivalence point. Accordingly, for rules near the equivalence point such as those shown in Fig. A1 (Rules # 34, 28, 31), the logic pursued approximate the equivalence point through small action over the control valve. In contrast, for those conditions far from the set point within the acidic region, a strong action was required in order to obtain a fast response of the valve action and get the process under control in a timely manner: i.e. Rules # 10, 1, 4, 7 and 16.

It is worth to mention that the experimental setup used through the research does not have an acid control valve to reject alkaline disturbances. As illustrated in Fig. A1 when the pH value is larger than pH = 7, the controller just can close the valve and let the acidic stream to lead the neutralization process. Such fact means that basic disturbances have not been considered during the research, and consequently, it is expected that the integral action never gets positive values (i.e. integral action corresponding to basic disturbances). As a result, for the experimental conditions covered there are 21 rules that are never used by the controller.

Once a first approximation to the 63 rules has been obtained, the available data for all the experimental runs covered in this work and the information about the rules utilization provided by the LabVIEW® software used to implement the controller are used for the heuristic optimization. The flow diagram shown in Fig. A2 depicts the tuning procedure followed during the research.

References

[1] M.J. Piovoso, J.M. Williams, Self-tuning pH control – a difficult problem, an effective solution, Instrum. Technol. 32 (1985) 45–49.
[2] D.E. Seborg, T.F. Edgar, S.L. Shah, Adaptive-control strategies for process-control – a survey, AIChE J. 32 (1986) 881–913.
[3] R.R. Rhinehart, Waste-water pH control, INTECH 37 (1990) 42–44.
[4] G.L. Williams, R.R. Rhinehart, J.B. Riggs, In-line process-model-based control of waste-water pH using dual base injection, Ind. Eng. Chem. Res. 29 (1990) 1254–1259.
[5] S. Engell, T. Heckenthaler, Fuzzy control-an alternative to model-based control? Methods of model based process control, in: Proceedings of the NATO Advanced Study Institute, 1995.
[6] T. Gustafsson, K. Waller, Dynamic modeling and reaction invariant control of pH, Chem. Eng. Sci. 38 (1983) 389–398.
[7] A.D. Kalafatis, L.P. Wang, W.R. Cluett, Linearizing feedforward-feedback control of pH processes based on the Wiener model, J. Process Control. 15 (2005) 103–112.
[8] T.K. Gustafsson, K.V. Waller, Nonlinear and adaptive-control of pH, Ind. Eng. Chem. Res. 31 (1992) 2681–2693.
[9] T.K. Gustafsson, B.O. Skrifvars, K.V. Sandstrom, K.V. Waller, Modeling of pH for control, Ind. Eng. Chem. Res. 34 (1995) 820–827.
[10] M.C. Palancar, J.M. Aragon, J.A. Miguens, J.S. Torrecilla, Application of a model reference adaptive control system to pH control. Effects of lag and delay time, Ind. Eng. Chem. Res. 35 (1996) 4100–4110.
[11] M.C. Palancar, J.M. Aragon, J.S. Torrecilla, pH-control system based on artificial neural networks, Ind. Eng. Chem. Res. 37 (1998) 2729–2740.
[12] M. Fuente, C. Robles, O. Casado, R. Tadeo, Fuzzy control of a neutralization process, IEEE, New York, NY, 2002.
[13] M. Adroer, A. Alsina, J. Aumatell, M. Poch, Wastewater neutralization control based on fuzzy logic: experimental results, Ind. Eng. Chem. Res. 38 (1999) 2709–2719.
[14] N.D. Ramirez-Beltran, H. Jackson, Application of neural networks to chemical process control, Comput. Ind. Eng. 37 (1999) 387–390.
[15] M.M. Mwembeshi, C.A. Kent, S. Salhi, A genetic algorithm based approach to intelligent modelling and control of pH in reactors, Comput. Chem. Eng. 28 (2004) 1743–1757.
[16] S. Syafiie, F. Tadeo, E. Martinez, Model-free learning control of neutralization processes using reinforcement learning, Eng. Appl. Artif. Intell. 20 (2007) 767–782.
[17] L.A. Zadeh, Fuzzy sets, Inf. Control. 8 (1965) 338.
[18] L.A. Zadeh, Outline of a new approach to analysis of complex systems and decision processes, IEEE Trans. Syst. Man Cybern. SMC3 (1973) 28–44.
[19] E.H. Mamdani, Applications of fuzzy set theory to control systems: a survey, in: M.M. Gupta, G.N. Saridis, B.R. Gaines (Eds.), Fuzzy Automata and Decision Processes, Elsevier Ltd., New York, 1977, pp. 77–88.
[20] C.L. Chen, P.C. Chen, C.K. Chen, Application of fuzzy adaptive controller in nonlinear process-control, Chem. Eng. Commun. 123 (1993) 111–126.
[21] R. Garrido, M. Adroer, M. Poch, Wastewater neutralization control based in fuzzy logic: simulation results, Ind. Eng. Chem. Res. 36 (1997) 1665–1674.
[22] B. Kelkar, B. Postlethwaite, Enhancing the generality of fuzzy relational models for control, Fuzzy Sets Syst. 100 (1998) 117–129.
[23] F.J. Molina, C. Leon, M.C. Arnaiz, J. Lebrato, Application of fuzzy logic for on-line control of a laboratory-scale anaerobic reactor, Appl. Sci. Environ. (1998) 23–31.
[24] O. Aras, M. Bayramoglu, A.S. Hasiloglu, Optimization of scaled parameters and setting minimum rule base for a fuzzy controller in a lab-scale pH process, Ind. Eng. Chem. Res. 50 (2011) 3335–3344.
[25] M.C. Palancar, L. Martin, J.M. Aragon, J.V. Briongos, PD and PID fuzzy logic controllers. Application to neutralization processes, in: R. Gani, K. Dam-Johansen (Eds.), European Congress of Chemical Engineering – 6, 2007, p. T4-8P.
[26] Z.A. Lotfi, Fuzzy Controllers Handbook, Newnes, Oxford, 1997.
[27] S. Chiu, Fuzzy model identification based on cluster estimation, J. Intell. Fuzzy Syst. 2 (1994) 267–278.
[28] S. Theodoridis, K. Koutroumbas, Pattern Recognition, Academic Press, San Diego, USA, 2003.